Available online at www.sciencedirect.com
ScienceDirect
Bioorganic & Medicinal Chemistry 15 (2007) 3463–3473
Bioorganic & Medicinal Chemistry

Synthesis, docking studies and anti-inflammatory activity of 4,5,6,7-tetrahydro-2*H*-indazole derivatives

Ornelio Rosati,[a,*] Massimo Curini,[a] Maria Carla Marcotullio,[a] Antonio Macchiarulo,[a] Marina Perfumi,[b] Laura Mattioli,[b] Francesco Rismondo[b] and Giancarlo Cravotto[c]

[a]*Dipartimento di Chimica e Tecnologia del Farmaco, Via del liceo 1, University of Perugia, 06123 Perugia (PG), Italy*
[b]*Dipartimento di Medicina Sperimentale e Sanità Pubblica, Università di Camerino Via Scalzino 3, 62032 Camerino (MC), Italy*
[c]*Dipartimento di Scienza e Tecnologia del Farmaco, Via P. Giuria 9, University of Torino, 10125 Torino (TO), Italy*

Received 12 December 2006; revised 28 February 2007; accepted 2 March 2007
Available online 6 March 2007

Abstract—A regioselective synthesis of 2,3-disubstituted tetrahydro-2*H*-indazols, mediated by α-zirconium sulfophenylphosphonate-methanephosphonate, was reported. Docking studies into the catalytic site of COX-2 were used to identify potential anti-inflammatory lead compounds. Two lead derivatives were chosen endowed with good binding energies and good ADME profiling. The biological in vivo evaluation of these compounds in two different experimental models (Freund's adjuvant-induced arthritis and carrageenan-induced oedema) proved the presence of anti-inflammatory activity. Noteworthy, both compounds evidenced the lack of any gastric injury even at high doses in gastric ulcerogenic assays.

1. Introduction

The pyrazole skeleton constitutes an important central template for a wide variety of biologically active compounds,[1] such as anti-microbial (**1**),[2] antiviral (**2**),[3] anti-inflammatory (**3**),[4] antidepressant (**4**),[5] anti-hyperglycaemic (**5**)[6] and pesticidal activity (**6**).[7]

In particular some of pyrazole derivatives were in depth investigated as nonsteroidal anti-inflammatory drugs (NSAIDs). The mechanism of action of this class of compounds is linked to the nonselective or selective inhibition of two cyclooxygenase isoforms, namely COX-1 and COX-2.[8] While COX-1 is a constitutive enzyme and is necessary for the proper function of the kidney and stomach through the synthesis of prostaglandins, COX-2 is an inducible form of the enzyme that mediates the inflammatory processes.[9]

The selective inhibition of COX-2 avoids the presence of gastrointestinal and renal side effects associated with the inhibition of the production of prostaglandins by COX-1.[10] Thus, COX-2 is a validated molecular target whose selective inhibition is sought in the development of anti-inflammatory therapies (Fig. 1).

The presence of a pyrazole nucleus is a common feature in the chemical structure of several COX-2 inhibitors. In particular, it consists in five- or six-membered carbocyclic or heterocyclic central template which is 1,2-disubstituted by aryl moieties. Two of the most known COX-2 selective inhibitors containing a pyrazole moiety are celecoxib (**7**, Celebrex)[11] and SC-558 (**8**).[11]

Recently, it has been reported that the cycloalkanopyrazole nucleus with a 1,3-diaryl substituted pattern (**9a**–**c**) is also a suitable scaffold for the development of selective COX-2 inhibitors.[4b]

The synthesis of this class of compounds relies on synthetic methodologies that use the pyrazole nucleus as starting building block.[4b,12,13] In searching for more general and versatile synthetic methodologies to prepare cycloalkanopyrazole derivatives, we recently reported that the use of a heterogeneous catalyst, such as layered zirconium sulfophenylphosphonate methanephosphonate [α-$Zr(CH_3PO_3)_{1,2}(O_3PC_6H_4SO_3H)_{0,8}$],[14] can be very useful for the synthesis of both pyrazole and 4,5,6,7-tetrahydro-1(2)*H*-indazole derivatives (1,2-

Keywords: Tetrahydro-2*H*-indazoles; Anti-inflammatory activity; Docking studies.
* Corresponding author. Tel.: +39 075 5855103; fax: +39 075 5855116; e-mail: ornros@unipg.it

0968-0896/$ - see front matter © 2007 Elsevier Ltd. All rights reserved.
doi:10.1016/j.bmc.2007.03.006

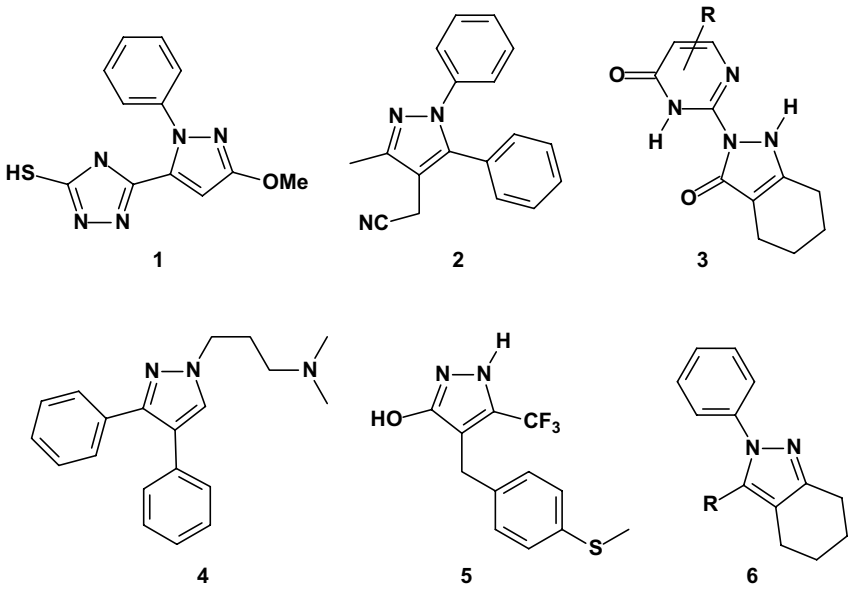

Figure 1. Some representative examples of active compounds containing a pyrazole moiety.

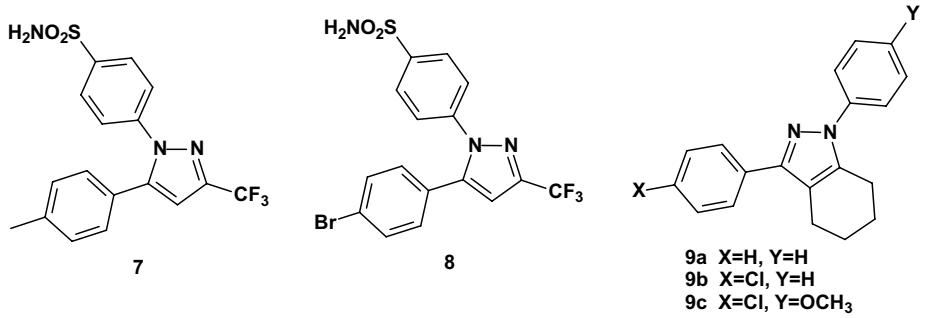

disubstituted cycloalkanopyrazole), starting from hydrazine and 1,3-diketones (Scheme 1).[15] In particular, this methodology has proven to be particularly effective towards the use of less reactive hydrazine such as 2,4-dinitrophenylhydrazine.

With the aim of developing novel anti-inflammatory lead compounds based on the selective inhibition of COX-2 enzyme and as a continuation of our ongoing effort in the field of pyrazole derivatives, we afforded the regio-selective synthesis of 2,3-disubstituted-4,5,6,7-tetrahydro-2*H*-indazoles (1,2-diarylcycloalkanopyrazoles). The preparation, molecular modelling studies and in vivo biological assays of this class of compounds are herein reported.

2. Chemistry

The synthesis of 2,3-diaryl-4,5,6,7-tetrahydro-2*H*-indazoles somewhat demanding and can be affected by isomer mixture formation,[4a] low/medium reaction yield.[13a,3c] or expensive reagents.[13b]

We found that α-zirconium sulfophenylphosphonate-methanephosphonate [α-$Zr(CH_3PO_3)_{1,2}(O_3PC_6H_4SO_3H)_{0,8}$] is an effective catalyst for the regioselective synthesis of 2,3-diaryl-4,5,6,7-tetrahydro-2*H*-indazole derivatives (Scheme 2).

The 2,3-diaryl-4,5,6,7-tetrahydro-2*H*-indazoles **10**–**15** were synthesized starting from 2-benzoylcyclohexanone and substituted hydrazines in the presence of α-$Zr(CH_3PO_3)_{1,2}(O_3PC_6H_4SO_3H)_{0,8}$ as the catalyst, in solvent-free and mild conditions. The adducts **10**–**15** were obtained with high yield as single isomer (Table 1). ^{1}H NMR experiments, such as NOESY, were carried out to establish the 1,2-disubstitution of the synthesized compounds.

For this purpose, we considered the possibility to observe NOE correlation between the aromatic substituents

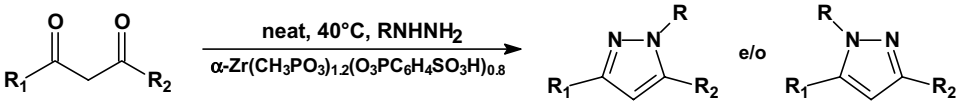

Scheme 1. Synthesis of Pyrazole derivatives mediated by zirconium sulfophenylphosphonate methanephosphonate.

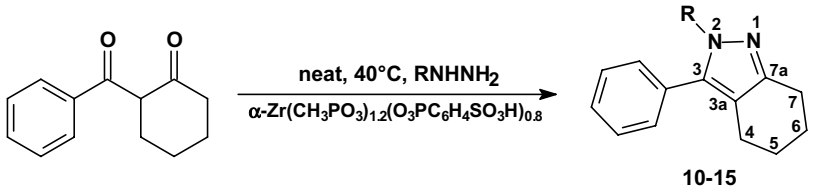

Scheme 2. Synthesis of 2,3-disubstituted tetrahydro-2*H*-indazole derivatives mediated by zirconium sulfophenylphosphonate methanephosphonate.

Table 1. Reaction of 2-benzoylcyclohexanones with hydrazines in the presence of α-$Zr(CH_3PO_3)_{1,2}(O_3PC_6H_4SO_3H)_{0,8}$

Compound	Hydrazines	Yield (%)	Time (h)
10	Phenylhydrazine	96	2
11	2-Hydrazino-4-(trifluoromethyl)pyrimidine	95	5
12	4-(Trifluoromethyl)phenylhydrazine	92	6
13	Methyl hydrazinecarboxylate	95	18
14	2-Hydrazinopyridine	81	12
15	2,5-Difluorophenylhydrazine	86	5

and the protons of the cyclohexane ring system (H-4 and H-7).

While it is possible to see the crosspeak of NOE correlation between the protons of the phenyl group on C-3 and the H-4, the lack of crosspeak of NOE correlation between the protons of the aromatic substituent on nitrogen and the H-7 is of a fundamental meaning for the assignment of 1,2-disubstitution in the synthesized compounds.

3. Results and discussion

A number of molecular docking experiments were carried out to identify potential COX-2 inhibitors among the class of 2,3-diaryl-4,5,6,7-tetrahydro-2*H*-indazoles (**10**–**15**). The resulting lead compounds were tested for their anti-inflammatory property in male Wistar rats (Harlan SRC, Milan, Italy), weighting 250–300 g, following two different experimental models: Freund's adjuvant-induced arthritis and carrageenan-induced oedema, both causing articular inflammation, frequently associated with erythema, swelling of periarticular tissues, enlargement and distortion of the joints, and involving limbs hardening and loss of limbs functionality. In addition, the selected lead compounds were evaluated for their anti-nociceptive activity and gastric ulcerogenic response.

3.1. Molecular docking experiments

To identify potential anti-inflammatory lead compounds among **10**–**15** endowed with COX-2 inhibition, docking calculations were performed using Autodock v3.0[16] into the 3D model of the catalytic site of COX-2 enzyme (pdb code: 1cx2).[17]

It should be mentioned that the Lamarckian genetic algorithm implemented in Autodock has been successfully employed to dock inhibitors into the catalytic site of the COX-2 and to well correlate the obtained binding free energies with inhibitory activities of compounds.[18] Briefly, we carried out comparative docking experiments of compounds **10**–**15** with known selective inhibitors of COX-2 such as SC-558 (**8**)[17] and a representative set of 1,3-diarylcycloalkanopyrazole derivatives (**9a**–**c**).[4b] The obtained results were evaluated in terms of binding energy and docking pose into the catalytic site of COX-2. Docking calculations predicted the binding conformation of SC-558 (**8**) with a root mean square deviation (RMSD) of 1.56 Å from the conformation obtained with X-ray crystallographic studies (Fig. 2). The high RMSD value observed between the predicted and the experimental bioactive conformation of SC-558 is ascribed to the different orientation that the sulfonamide group adopts in the docked conformation. However, several studies pinpoint that the sulfonamide group could bind at the enzyme in several conformations than suggested by the crystal structure.[17–19] In particular, Liu et al. quantified the energetic preference of the sulfonamide group of SC-558 binding at COX-2 as resulting from Autodock prediction.[18] The authors indicated that the predicted conformation was lower in energy than the observed conformation in the crystal structure of COX-2.

Table 2 shows the energetic scores of the top solutions found during docking experiments of compounds **8**–**15**. SC-558 (**8**) is endowed with the best binding energy among the studied compounds (−11.53 kcal/

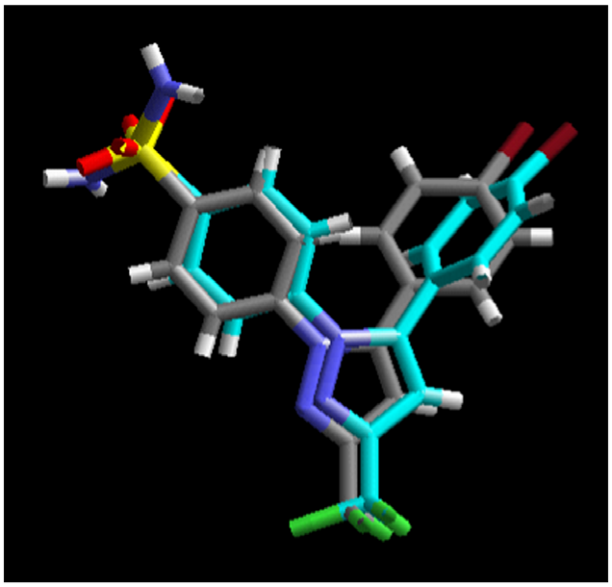

Figure 2. Superposition between the predicted conformation of SC-558 (**8**) from docking experiments (carbon atoms in cyan colour) and the crystallographic conformation (carbon atoms in grey colour).

Table 2. Binding energies of top scoring solutions as resulting from docking experiments

Compound	Binding energy (kcal/mol)	IC_{50} (μM)
8	−11.53	0.0093[a]
9a	−9.50	0.57[b]
9b	−9.96	0.62[b]
9c	−9.32	1.56[b]
10	−9.67	—
11	−10.59	—
12	−10.88	—
13	−9.06	—
14	−9.76	—
15	−10.26	—

[a] Activity data from Ref. 17.
[b] Activity data from Ref. 4b.

mol). Two compounds (**11** and **12**) out of six 2,3-disubstituted-cycloalkanopyrazoles display improved binding energies compared to the active 1,3-diarylcycloalkanopyrazole derivatives (**9a**–**c**) with a minimum difference of 0.63 kcal/mol between compounds **11** and **9b**.

The inspection of the obtained COX-2 complexes with SC-558 (**8**) and compounds **11** and **12** reveals binding poses located in the centre of the binding pocket of COX-2. In this binding mode, three anchor sites (P1, P2 and P3) can clearly be identified (Fig. 3).

The site P1 contains the recognition elements of the sulfonamide group of SC-558 (**8**) and the trifluoromethyl moiety of compounds **11** and **12**. In this pocket the amido group of sulfonamide moiety acts as an hydrogen bond donor with the backbone oxygen of Leu352 and the side-chain oxygen of Gln192, while one oxygen of the moiety acts as an hydrogen bond acceptor with the guanidine group of Arg513 (Fig. 4a).

The trifluoromethyl moiety of compounds **11** and **12** forms hydrogen bond interactions with the backbone of Ile517 and the amido group of Gln192 (Fig. 4b and c). These hydrogen-bonding interactions play a key role

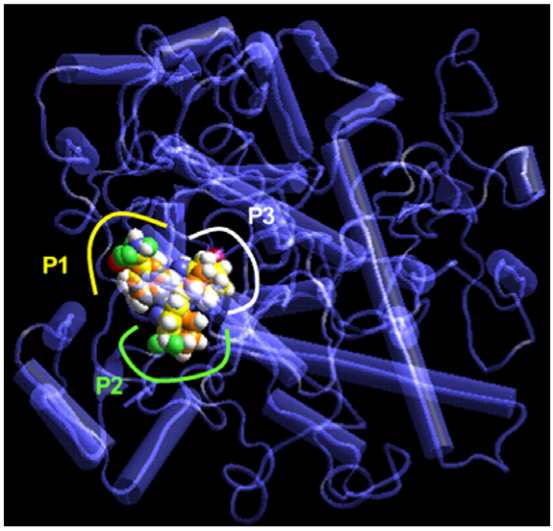

Figure 3. Anchor sites (P1, P2 and P3) of compounds SC-558 (**8**), **11** and **12** in the binding pocket of COX-2.

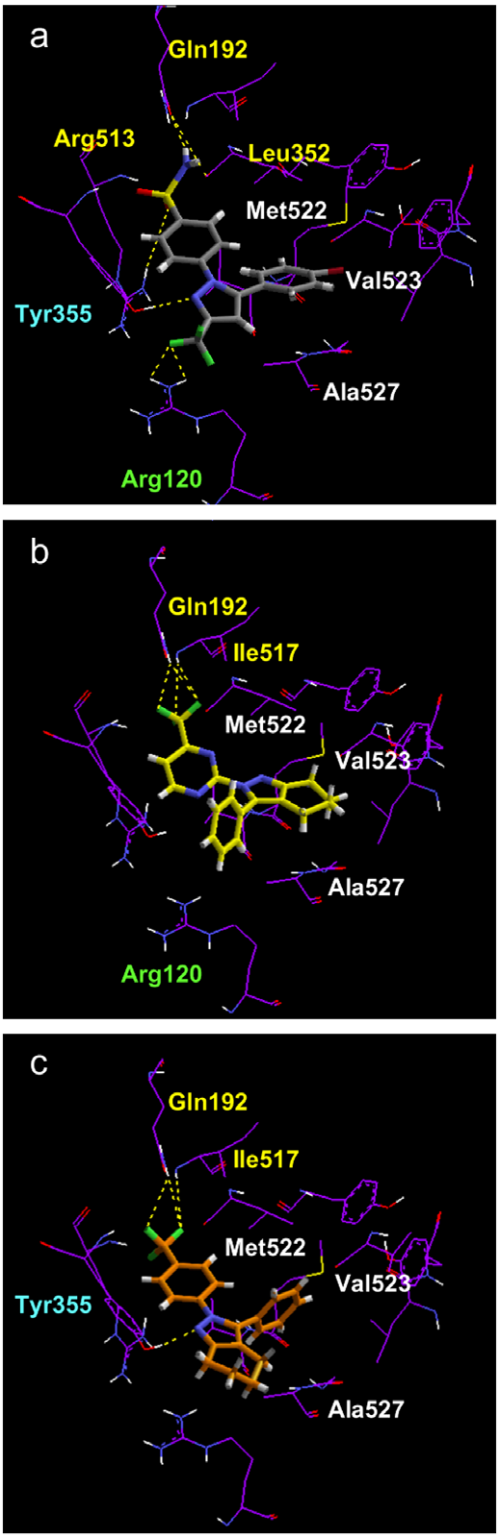

Figure 4. Residues involved in the interactions with compounds **8** (a), **11** (b) and **12** (c) in the binding site of COX-2 as resulting from docking experiments.

in determining the 3D space position of the cycloalkanopyrazole moieties in the binding pocket of COX-2.

Thus, the difference observed between the binding mode of the cycloalkanopyrazole moiety of compounds **11** and **12** is ascribed to the strong hydrogen-bonding inter-

action that the trifluoromethyl group of **11** forms in site P1. This interaction is more energetically favoured than the one resulting with the trifluoromethyl group occupying site P3. The occupancy of site P1 by the trifluoromethyl group hampers that the cycloalkanopyrazole moiety of compound **11** could assume a similar docking pose as observed in compound **12**.

The site P2 binds the trifluoromethyl group of SC-558, the phenyl group of compound **11** and the cycloalkanopyrazole moiety of **12**. While the trifluoromethyl group of SC-558 (**8**) acts as an hydrogen bond acceptor with the guanidine group of Arg120, the phenyl ring of compound **11** forms π–cation interaction with the positively charged side chain of Arg120. Conversely, hydrophobic interactions with the side-chain carbons of Arg120 stabilize the binding of the cycloalkanopyrazole moiety of compound **12** at site P2.

The anchor site P3 interacts with the *p*-bromo-phenyl moiety of SC-558, the cycloalkanopyrazole moiety of **11** and the phenyl ring of compound **12** through hydrophobic interactions that involve residues Met522, Val523 and Ala527.

The binding pose of SC-558 (**8**) and compound **12** is also enforced through an hydrogen bond interaction between the central pyrazole moiety and the hydroxyl group of Tyr355.

The bioavailability of compounds **10**–**15** was assessed using ADME (adsorption, distribution, metabolism, elimination) prediction methods. In particular, we calculated the compliance of compounds to the Lipinski's role of five.[20] Briefly, this simple role is based on the observation that most orally administered drugs have a molecular weight (MW) of 500 or less, a log *P* no higher than 5, five or fewer hydrogen bond donor sites and 10 or fewer hydrogen bond acceptor sites (N and O atoms). In addition, we calculated the polar surface area (PSA) since it is another key property that has been linked to drug bioavailability.[21] Thus, passively absorbed molecules with a PSA > 140 $Å^2$ are thought to have low oral bioavailabilities.[22]

On the basis of docking results (Table 2) and bioavailability scores (Table 3) we choose compounds **11** and **12**for in vivo evaluation of their anti-inflammatory activity. Compound **11** is the third ranked molecule in terms of binding energy with a difference of 1.0 kcal/mol from SC-558 (**8**). Compound **12** violates the role of five once with its log *P* value. However, since this violation is subtle, 0.49 U above the cut-off value of 5, and given its better binding energy within the series of 2,3-disubstituted-cycloalkanopyrazoles, we took this compound into account for in vivo biological assays.

Table 3. Compliance of compounds to computational parameters of bioavailability

Compound	No. of role of five violations	PSA ($Å^2$)
8	0	86.36
9a	0	17.82
9b	1 (log *P* = 5.45)	17.82
9c	1 (log *P* = 5.19)	27.05
10	0	17.82
11	0	43.60
12	1 (log *P* = 5.49)	17.82
13	0	44.12
14	0	30.71
15	0	17.82

3.2. Anti-inflammatory activity: Freund's adjuvant-induced arthritis

Freund's adjuvant-induced arthritis has been used as a model of sub-chronic or chronic inflammation in rats and it is of considerable relevance for the study of pathophysiological and pharmacological control of inflammatory processes, as well as the evaluation of potential analgesic or anti-inflammatory effects of drugs.[23,24] One of the reasons for the wide utilization of this model is due to the strong correlation between the efficiency of therapeutic agents in this model and in rheumatoid arthritis in humans. The arthritis is induced by a subplantar injection of 0.1 ml of Freund's adjuvant (complete fraction of *Mycobacterium butyricum* suspended in mineral oil; Sigma Chemical Co., USA) in the right paw's plantar surface. The adjuvant elicits arthritis predominantly in the joints of hind limbs, promoting significant reduction of motor activity and increased itching and scratching behaviours.[25]

All animals were subjected to assessment of body weight and measurements of the right paw (the width and height of the paw and width of the joints were measured with a caliper ruler) (baseline). Subsequently, Freund's adjuvant was injected in the right paw: 3 days after the administration (this period was established with preliminary tests and it is necessary for achieving a relevant inflammatory disease), the animals were subjected again to the measures to verify the arthritis development (day 0), and then they were randomly assigned to one of the experimental groups.

Starting from this day (day 0), rats were orally injected once daily for further 3 days (day 1, day 2, day 3) with compound **11** (10, 50, 100, 200 mg/kg/10 ml), compound **12** (10, 50, 100 mg/kg/10 ml) or vehicle (10% DMSO, 10% TWEEN 80, 80% distilled water).

Evaluation of the anti-inflammatory effects of tested compounds was performed on day 1, day 2, day 3 and on day 4 (the day after the last injection), by monitoring the width and height of the paw and the width of the joints in the right paw.

The same experimental procedure was carried out to test the anti-inflammatory activity of compound **11** (10, 50, 100, 200 mg/kg/2 ml), compound **12** (10, 50, 100 mg/kg/2 ml) or vehicle (10% DMSO, 10% TWEEN 80, 80% distilled water), after intraperitoneal injection.

The obtained results confirmed the ability of Freund's adjuvant administration to induce a severe inflammatory status in rat's hind paw. After a 4-day course of treatment, progression of inflammation was reversed,

depending on the dose and on the route of compounds administered.

Specifically, both oral and ip administration of higher doses of compound **11** reduced paw height [$F(3,20) = 3.898$; $p < 0.05$] and [$F(3,20) = 4.052$; $p < 0.05$], respectively, from the 3rd or 2nd treatment on (Fig. 5a–d), whereas paw width was significantly reduced by ip administration [$F(3,20) = 7.486$; $p < 0.01$] (Fig. 5e) but not by oral administration [$F(3,20) = 1.743$; $p > 0.05$] (Fig. 5b). Regarding joint width, either oral or ip injection of compound **11** was ineffective to decrease the joint size compared to vehicle group [$F(3,20) = 0.579$; $p > 0.05$] and [$F(3,20) = 1.400$; $p > 0.05$], respectively (Fig. 5c–f).

All doses of compound **12** were ineffective to reduce paw-oedema when orally administered (paw height, [$F(3,20) = 1.073$; $p > 0.05$]; paw width, [$F(3,20) = 0.081$; $p > 0.05$]; joint width, [$F(3,20) = 1.456$; $p > 0.05$]) (Fig. 6a–c, respectively). Instead ip administration of compound **12** (50, 100 mg/kg) significantly decreased

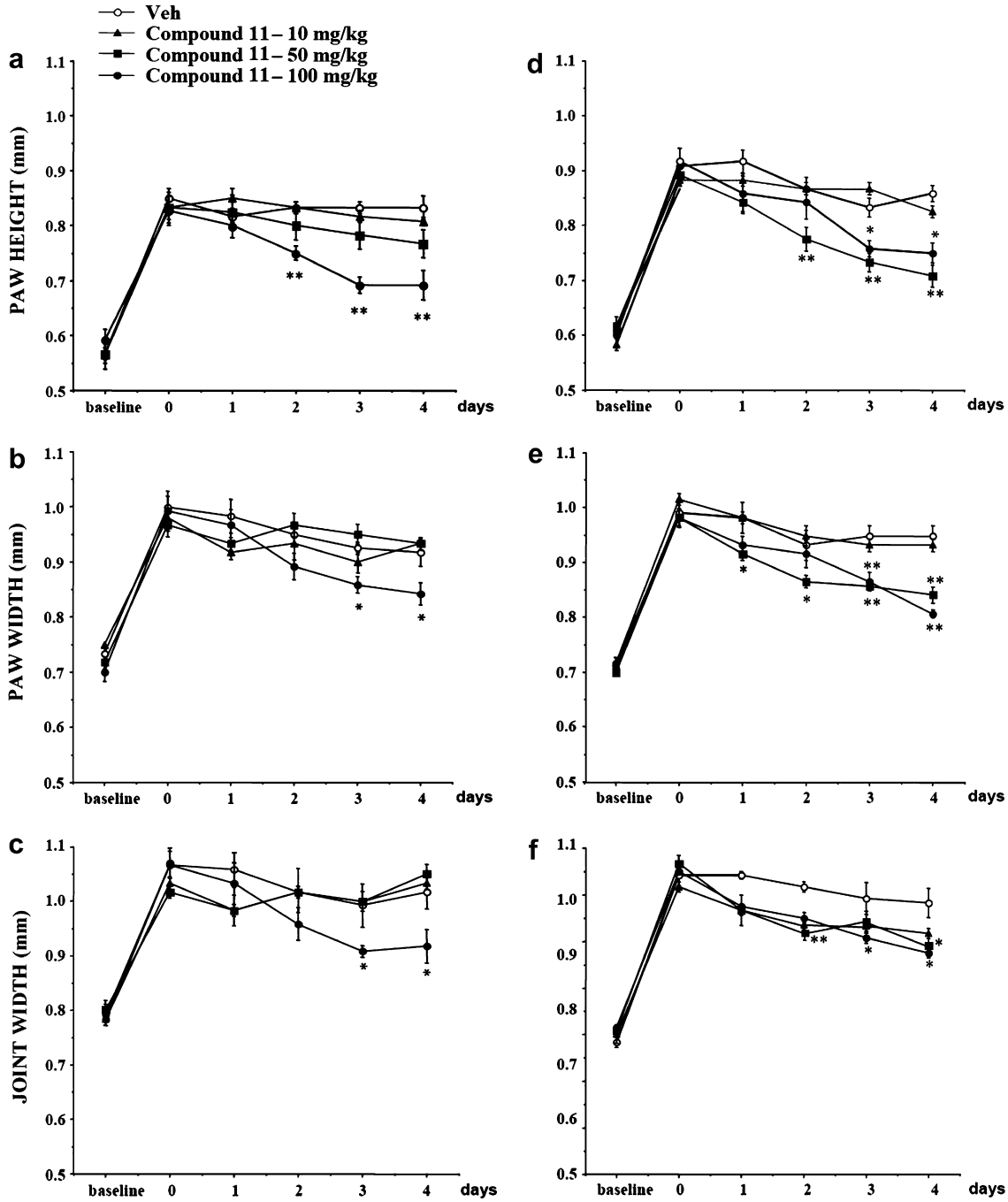

Figure 5. Anti-inflammatory activity of compound **11** on Freund's adjuvant-induced arthritis in rats. (a–c) and (d–f) represent the effect of, respectively, oral and ip administration of compound **11** (10, 50, 100 mg/kg) or vehicle on the different measurements of paw height, paw width and joint width, respectively, before (baseline) and after (day 0) arthritis-induction and throughout 4-day course of treatment (days 1–4). Values are expressed as means ± SEM. Difference from vehicle group: $^{*}p < 0.05$, $^{**}p < 0.01$, where not indicated, the difference was not statistically significant.

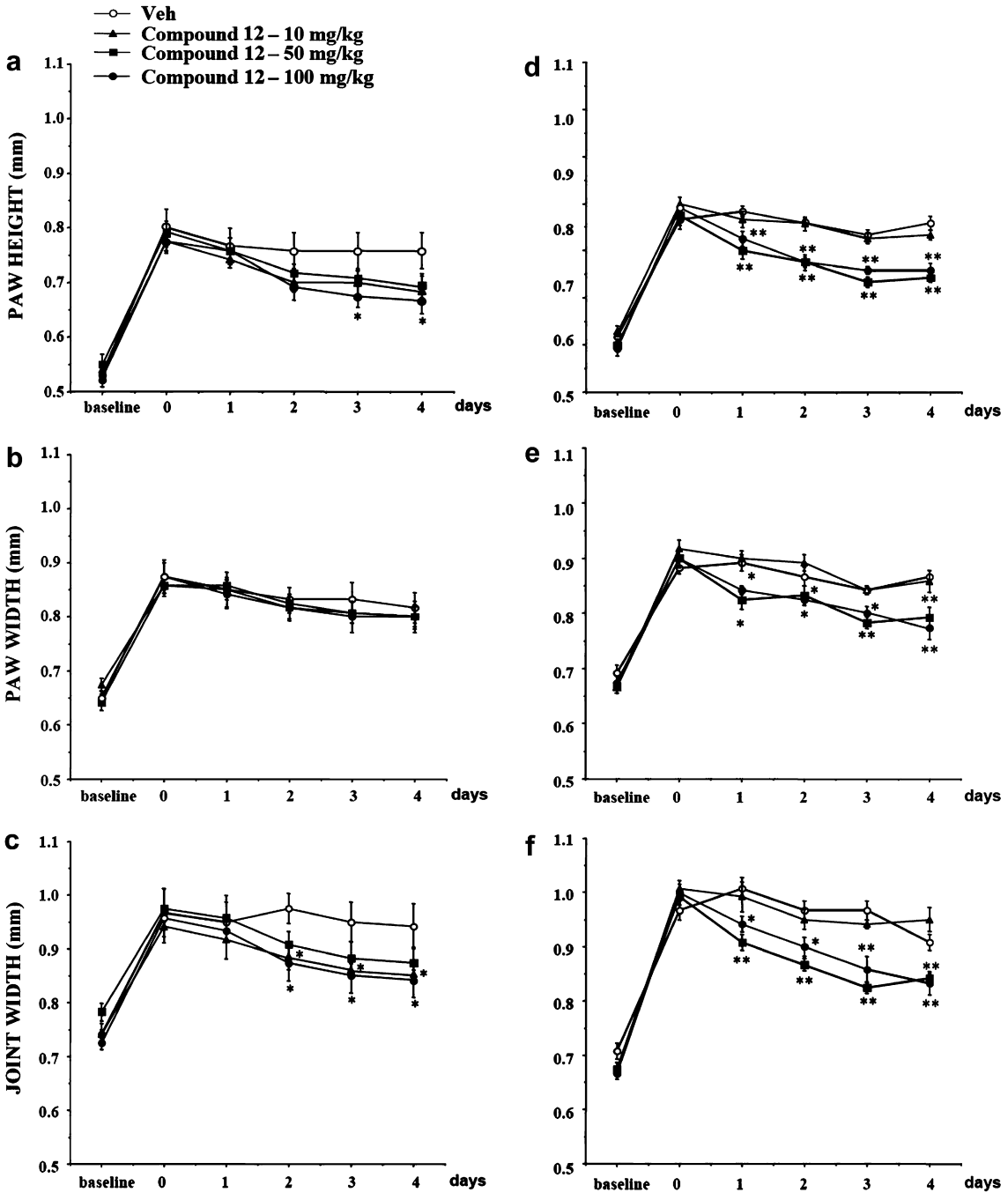

Figure 6. Anti-inflammatory activity of compound **12** on Freund's adjuvant-induced arthritis in rats. (a–c) and (d–f) represent the effect of, respectively, oral and ip administration of compound **12** (10, 50, 100 mg/kg) or vehicle on the different measurements of paw height, paw width and joint width, respectively, before (baseline) and after (day 0) arthritis-induction and throughout 4-day course of treatment (days 1–4). Values are expressed as means ± SEM. Difference from vehicle group: $^{*}p < 0.05$, $^{**}p < 0.01$, where not indicated, the difference was not statistically significant.

either paw height [$F(3,20) = 15.709$; $p < 0.001$], paw width [$F(3,20) = 8.770$; $p < 0.001$] and joint width [$F(3,20) = 13.725$; $p < 0.001$] from the 1st treatment on (Fig. 6d–f, respectively).

3.3. Anti-inflammatory activity: carrageenan-induced paw-oedema

Anti-inflammatory activity of lead compounds was also determined by carrageenan-induced paw-oedema.[26] Carrageenan is a polymeric irritant that induces an acute inflammatory response on injection into tissues. Injected into the footpad of rats it is known to cause physiological and biochemical changes leading to oedema limited to the affected limb,[27,28] over a short time course (maximal effect after 4–6 h).[29] Rats, fasted overnight, received orally compound **11** (10, 50, 100 mg/kg/10 ml), compound **12** (10, 50, 100 mg/kg/10 ml) or vehicle.

One hour later, paw-oedema was induced by injection of 0.1 ml of 1.0% λ carrageenan suspension in the sub-plantar region of the right hindpaw. An equivalent

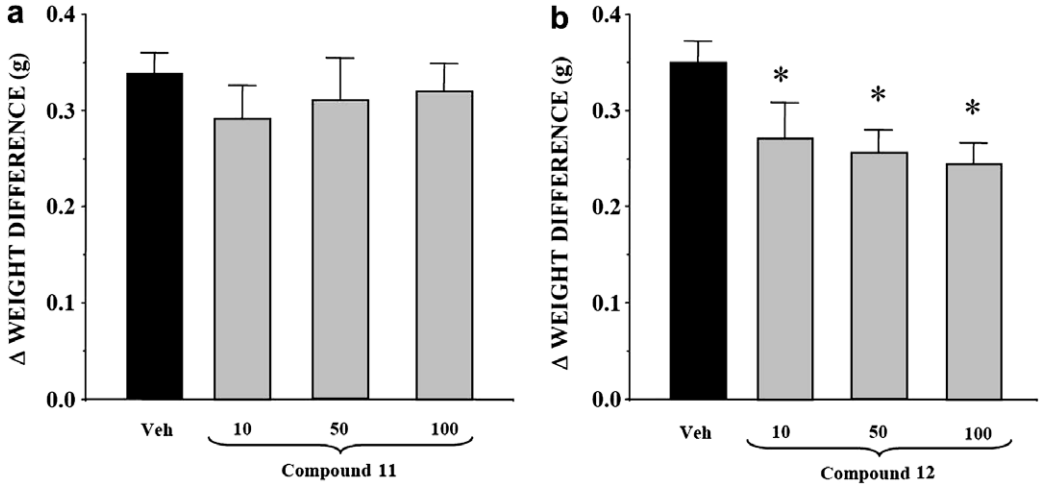

Figure 7. Anti-inflammatory activity of compound **11** (a) and compound **12** (b), orally administered, on carrageenan-induced paw-oedema in rats, expressed as weight difference of carrageenan-treated vs. vehicle-treated paw. Values are expressed as means ± SEM. Difference from vehicle group: $^{*}p < 0.05$, where not indicated, the difference was not statistically significant.

volume of saline solution was injected in the same region of the left hindpaw. Four hours later, animals were sacrificed and their hind paws cut and weighed.[30] The anti-inflammatory activity was evaluated by the weight difference of right vs. left paw. Results confirmed the ability of carrageenan injection to induce a marked inflammation on hindpaw of treated rats. All doses of compound **12** exhibited antiinflammatory properties, since this compound dose-dependently reduced carrageenan-induced paw-oedema compared with vehicle-treated rats [$F(3,20) = 3.750$; $p < 0.05$] (Fig. 7b), whereas compound **11** was ineffective to reduce paw-oedema at all doses tested [$F(3,20) = 0.956$; $p > 0.05$] (Fig. 7a).

3.4. Gastric ulcerogenic response

Gastroenteropathy is the most common side effect among patients taking NSAIDs for inflammatory disorders, especially rheumatoid arthritis. It has been reported that gastric mucosal lesions induced by conventional NSAIDs, such as indomethacin, naproxen and aspirin, were significantly aggravated in arthritis-affected rats when compared with normal rats.[31,32]

It has also been reported that the selective COX-2 inhibitors such as rofecoxib and celecoxib, even at a higher dose (100 mg/kg), did not induce any damage in normal rat stomachs but caused gross lesions in the stomach of arthritic rats.[32]

Taking into consideration this side effect, we investigated the influence of our compounds on the integrity of gastric mucosa in rats with adjuvant-induced arthritis and compared the effects with those of indomethacin, a conventional NSAID.

Therefore, arthritis was induced in rats as reported above. Two days later, they were fasted overnight and, the day after, orally administered with compound **11** (10, 50, 100 mg/kg/10 ml), compound **12** (10, 50, 100 mg/kg/10 ml) or vehicle. Another group of rats received orallyfast indomethacin (10 mg/kg/5 ml) as positive controls.[31] Four hours later, rats were killed and their stomachs removed and opened along the greater curvature. The ulcerative index (UI) was expressed as the sum of the lengths (mm) of lesions found in the mucosal membrane.[33]

Oral administration of indomethacin (10 mg/kg) caused severe haemorrhagic lesions in the gastric mucosa of arthritic rats (UI = 40.833 ± 1.6). In contrast, neither compound **11** [$F(3,20) = 614.290$; $p < 0.01$] nor compound **12** [$F(3,20) = 618.814$; $p < 0.01$] induced any damage in the stomach of arthritic rats, even at the highest dose of 100 mg/kg.

3.5. Anti-nociceptive activity

In arthritis-affected rats the anti-nociceptive activity of compound **12** was also evaluated using the hot plate test.[34] The apparatus consists of a 20-cm diameter metal hot-plate surface (Basile, Milan, Italy) set at 55 ± 0.5 °C to give a latency-time of 15–18 s in control group.

Pain threshold was determined by the latency for nociceptive response (licking of any hind paw or jump) with a maximum cut-off time of 60 s. Arthritis-affected rats (see above) were ip administered once daily for 4 days with compound **12** (10, 50, 100 mg/kg/10 ml) or vehicle. The day after the last injection, rats were tested twice, 30 min apart. A group of normal rats was added as positive controls.

As shown in Figure. 8, arthritis-affected rats exhibited a latency time for nociceptive response lower than that of normal rats [$F(1,10) = 24.694$; $p < 0.01$], corresponding to augmented sensitivity to pain. Intraperitoneal administration of compound **12** at doses of 50, 100 mg/kg/10 ml increased the latency time for nociceptive response compared to vehicle-treated arthritis rats, but the difference was not statistically significant [$F(3,20) = 2.298$; $p > 0.05$].

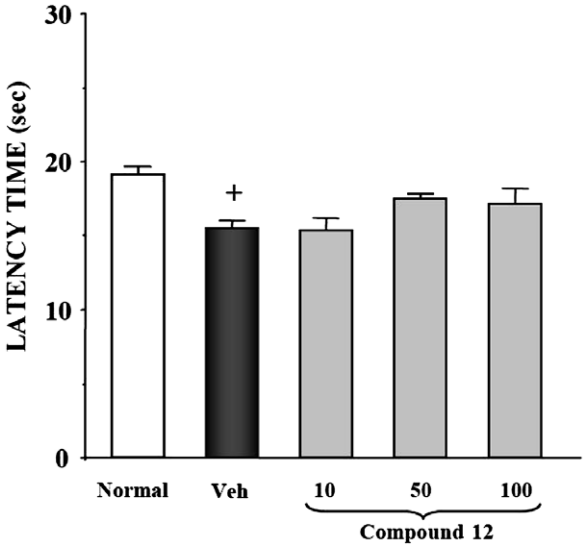

Figure 8. Anti-nociceptive activity of compound **12** (10, 50, 100 mg/kg ip) in hot-plate test in rats, expressed as latency time for nociceptive response of arthritis-affected rats compared to normal rats. Values are expressed as means ± SEM. Difference from normal-group: $^{+}p < 0.05$, where not indicated, the difference was not statistically significant.

4. Conclusion

Molecular docking calculations followed by a number of in vivo biological assays were used to identify novel anti-inflammatory agents among the class of 2,3-diaryl-4,5,6,7-tetrahydro-2*H*-indazoles (**10**–**15**) and acting through a COX-2 inhibition mechanism.

The obtained results indicate that both compounds **11** and compound **12** possess significant anti-inflammatory activity both after oral and intraperitoneal administration.

In Freund's adjuvant-induced arthritis model, both compounds are able to reduce the progression of inflammation, but their anti-inflammatory activity is better after ip than oral administration, probably due to a lower bioavailability following a reduced absorption or to an increased metabolism of tested-compounds when orally administered.

After ip injection, compound **12** showed a dose-dependent ready and steady effect, whereas at the same doses, compound **11** exhibited a late and less effective effect.

Moreover, the difference in the anti-inflammatory activity of the two compounds is highlighted by the carrageenan-induced oedema test, where only the compound **12** reduced paw-oedema at all doses tested contrary to compound **11** that was ineffective.

In conclusion, the results of this study show that compound **12**, more than compound **11**, exhibits anti-inflammatory activity against adjuvants-induced arthritis, and against early phase of inflammation (acute paw-oedema), without any deleterious side effects. Indeed both compounds show a lack of gastric injury even at high doses.

5. Experimental methods

5.1. General remarks

All chemicals were purchased from the major chemical suppliers as highest purity grade and used without any further purification. Column chromatography was performed with Merk silica gel 60 (70–230 mesh ASTM), with hexane/ethyl acetate mixture. ^{1}H and ^{13}C NMR were recorded in $CDCl_3$ with a Brucker Avance DRX 200 spectrometer at a frequency of 200.1 and 50 MHz, respectively, or Brucker Avance DPX 400 spectrometer at a frequency of 400.13 and 100.62 MHz, respectively. Chemical shifts (δ) are reported in ppm relative to TMS; *J* values are given in Hz. GC-MS analysis was performed with an HP-6890 gas chromatograph (dimethyl silicone column, 12.5 m) equipped with an HP-5973 mass-selective detector at an ionizing voltage of 70 eV. Melting points are uncorrected. Reported yields are for isolated compounds judged pure by NMR analysis.

5.2. Typical reaction procedure

To the mixture of 2-benzoylcyclohexanone (1 mmol) and α-$Zr(CH_3PO_3)_{1.2}(O_3PC_6H_4SO_3H)_{0.8}$ (25 mg, ~6% molar), under stirring, under nitrogen and in neat, hydrazine derivative (1 mmol) was added. The mixture was left to react at 50 °C and monitored by TLC. The reaction mixture was diluted with dichloromethane, filtered on buckner and then concentrated under vacuum. The structures of 2,3-diaryl-4,5,6,7-tetrahydro-2*H*-indazoles were determined on the basis of the typical ^{1}H NMR chemical shifts and NOESY experiments.

5.3. 2,3-Diphenyl-4,5,6,7-tetrahydro-2*H*-indazole (10).[13c]

Yield, 96%; white powder; mp 107–108 °C; ^{1}H NMR (400 MHz, $CDCl_3$) δ 1.81 (m, 2H, CH_2), 1.91 (m, 2H, CH_2), 2.62 (t, $J = 6.1$ Hz, 2H, CH_2), 2.84 (t, $J = 6.1$ Hz, 2H, CH_2), 7.29 (m, 10H, ArH); ^{13}C NMR (50 MHz, $CDCl_3$) δ 21.5, 23.3, 23.4, 23.5, 116.1, 124.8, 126.6, 127.7, 128.4, 128.7, 129.2, 130.8, 138.4, 140.4, 150.3; GC–MS *m*/*z* 274 (M^+), 257, 246, 231, 218, 180, 153, 128, 115, 77.

5.4. 3-Phenyl-2-[4-(trifluoromethyl)pyrimidin-2-yl]-4,5,6,7- tetrahydro-2*H*-indazole (11)

Yield, 95%; white powder; mp 97–98 °C; ^{1}H NMR (400 MHz, $CDCl_3$) δ 1.78 (m, 2H, CH_2), 1.90 (m, 2H, CH_2), 2.53 (t, $J = 6.3$ Hz, 2H, CH_2), 2.90 (t, $J = 6.3$ Hz, 2H, CH_2), 7.26 (m, 3H, ArH), 7.37 (m, 3H, ArH), 8.92 (d, $J = 4.8$ Hz, 1H, ArH); ^{13}C NMR (100 MHz, $CDCl_3$) δ 21.3, 23.3, 23.4, 24.1, 113.4, 120.0 (q, $J_{CF} = 274.2$ Hz), 120.7, 128.19, 128.23, 129.3, 131.9, 141.3, 154.3, 156.7 (q, $J_{CF} = 37.2$ Hz), 157.7, 161.5; GC–MS *m*/*z* 344 (M^+), 316, 290, 275, 197, 147, 77.

5.5. 3-Phenyl-2-[4-(trifluoromethyl)phenyl]-4,5,6,7-tetrahydro-2*H*- indazole (12)

Yield, 92%; white powder; mp 104–105 °C; ^{1}H NMR (400 MHz, $CDCl_3$) δ 1.81 (m, 2H, CH_2), 1.92 (m, 2H, CH_2), 2.60 (t, J = 6.1 Hz, 2H, CH_2), 2.84 (t, J = 6.1 Hz, 2H, CH_2), 7.21 (d, J = 6 Hz, 2H, PhH), 7.37 (m, 5H, PhH), 7.54 (d, J = 6 Hz, 2H, PhH); ^{13}C NMR (100 MHz, $CDCl_3$) δ 21.6, 23.5, 23.6, 23.8, 118.3, 126.9 (q, J_{CF} = 270.4 Hz), 124.4, 126.2 (q, J_{CF} = 4.0 Hz), 128.5, 129.0, 129.5, 130.8, 138.9, 143.4, 151.6; GC–MS *m*/*z* 342 (M^+), 314, 265, 248, 197, 145, 77.

5.6. Methyl-3-phenyl-4,5,6,7-tetrahydro-2*H*-indazole-2-carboxylate (13)

Yield, 95%; white powder; mp 85–86 °C; ^{1}H NMR (400 MHz, $CDCl_3$) δ 1.73 (m, 2H, CH_2), 1.84 (m, 2H, CH_2), 2.42 (t, J = 6.2 Hz, 2H, CH_2), 2.79 (t, J = 6.2 Hz, 2H, CH_2), 3.92 (s, 3H, OCH_3), 7.29–7.47 (m, 5H, PhH); ^{13}C NMR (50 MHz, $CDCl_3$) δ 20.7, 22.7, 22.8, 23.7, 54.2, 120.4, 127.9, 128.4, 129.1, 130.6, 141.9, 150.5, 154.1; GC–MS *m*/*z* 256 (M^+), 241, 265, 228, 197, 169, 141, 77.

5.7. 3-Phenyl-2-pyridin-2-yl-4,5,6,7-tetrahydro-2*H*-indazole (14)

Yield, 81%; yellow powder; mp 137–138 °C; ^{1}H NMR (200 MHz, $CDCl_3$) δ 1.73–2.09 (m, 4H, 2× CH_2), 2.63 (t, J = 6 Hz, 2H, CH_2), 2.87 (t, J = 6 Hz, 2H, CH_2), 7.13–7.26 (m, 7H, ArH + PyH), 7.70 (td, J = 1.9, 8 Hz, 1H, PyH), 8.38 (dd, J = 1.5, 5.6 Hz, 1H, PyH); ^{13}C NMR (100 MHz, $CDCl_3$) δ 21.7, 23.5, 23.7, 23.9, 118.2, 118.5, 121.9, 127.9, 128.5, 129.3, 131.5, 138.1, 139.1, 148.8, 151.7, 152.9; GC–MS *m*/*z* 275 (M^+), 246, 219, 197, 169, 115, 77.

5.8. 2-(2,5-Difluorophenyl)-3-phenyl-4,5,6,7-tetrahydro-2*H*-indazole (15)

Yield, 86%; white powder; mp 125–126 °C; ^{1}H NMR (200 MHz, $CDCl_3$) δ 1.75–2.04 (m, 4H, 2× CH_2), 2.67 (t, J = 6 Hz, 2H, CH_2), 2.85 (t, J = 6 Hz, 2H, CH_2), 7.03 (m, 2H, ArH), 7.17–7.42 (m, 6H, ArH); ^{13}C NMR (100 MHz, $CDCl_3$) δ 21.7, 23.4, 23.7, 23.8, 115.9 (d, J_{CF} = 25.5 Hz), 116.2 (dd, J_{CF} = 23.6, 7.7 Hz), 116.6, 117.6 (dd, J_{CF} = 31.9, 9.2 Hz), 128.3, 128.6, 128.7, 129.7 (dd, J_{CF} = 13.8, 10.5 Hz), 130.4, 140.6, 151.8, 152.8 (d, J_{CF} = 246.7 Hz), 158.5 (d, J_{CF} = 243.1 Hz); GC–MS *m*/*z* 310 (M^+), 282, 233, 197, 170, 140, 113, 77.

5.9. Molecular modelling

Docking experiments were performed using Autodock v3.0.[16] Ligands were built using the sketch module of Cerius-2.[35] Each compound was minimized using the Universal force-field v.1.2 and the Smart Minimizer protocol of the Open Force Field module (OFF).[36] Atomic charges were calculated using the semi-empirical Mopac/AM1 method for small molecules. Atomic charges of residues were calculated using the Kollman united charge model of the Amber force field as implemented in Autodock tools package.[37] Each docking experiment consisted in 100 docking runs using the genetic algorithm with a population size of 50 individuals and 2,500,000 energy evaluations. Other parameters were left to their respective default values. The search was conducted in a grid of 60 points per dimension and a step size of 0.375 centred on the binding site of SC-558 as resulting from the crystallized complex with COX-2 (pdb code 1cx2).[17] Role of five violations and polar surface area (PSA) were calculated using JChem.[13,38] All calculations were carried out on SGI O2 R5000 and R10000 workstations.

Acknowledgements

Financial support from MIUR, National Project "Sviluppo di processi ecocompatibili nella sintesi organica" and CEMIN (Centro di Eccellenza Materiali Innovativi Nanostrutturati per applicazioni chimiche, fisiche e biomediche) is gratefully acknowledged.

References and notes

1. (a) Elguero, J.. In *Comprehensive Heterocyclic Chemistry*; Katritaky, A. R., Rees, C. W., Eds.; Pergamon: Oxford, 1984; Vol. 5, p 167; (b) Elguero, J. In *Comprehensive Heterocyclic Chemistry II*; Katritaky, A. R., Rees, C. W., Scriven, E. F., Eds.; Elsevier: Oxford, 1996; Vol. 3, pp 1–75.
2. Mahajan, R. N.; Havaldar, F. H.; Fernandes, P. S. *J. Indian Chem. Soc.* **1991**, *68*, 245.
3. (a) Genin, M. J.; Biles, C.; Keiser, B. J.; Poppe, S. M.; Swaney, S. M.; Tarpley, W. G.; Yagi, Y.; Romero, D. L. *J. Med. Chem.* **2000**, *43*, 1034; (b) Janus, S. L.; Magdif, A. Z.; Erik, B. P.; Claus, N. *Monatsh. Chem.* **1999**, *130*, 1167.
4. (a) Badawey, E.; El-Ashmawey, I. M. *Eur. J. Med. Chem.* **1998**, *33*, 349; (b) Sui, Z.; Guan, J.; Ferro, M. P.; McCoy, K.; Wachter, M. P.; Murray, W. V.; Singer, M.; Steber, M.; Ritchie, D. M.; Argentieri, D. C. *Bioorg. Med. Chem. Lett.* **2000**, *10*, 601.
5. Bailey, D. M.; Hansen, P. E.; Hlavac, A. G.; Baizman, E. R.; Pearl, J.; Defelice, A. F.; Feigenson, M. E. *J. Med. Chem.* **1985**, *28*, 256.
6. Kees, K. L.; Fitzgerald, J. J.; Steiner, K. E.; Mattes, J. F.; Mihan, B.; Tosi, T.; Mondoro, D.; McCaleb, M. L. *J. Med. Chem.* **1996**, *39*, 3920.
7. Lyga, J. W.; Patera, R. M.; Plummer, M. J.; Halling, B. P.; Yuhas, D. A. *Pestic. Sci.* **1994**, *42*, 29.
8. Xie, W.; Chipman, J.; Robertson, D. L.; Erikson, R. L.; Simmons, D. L. *Proc. Natl. Acad. Sci. U.S.A.* **1991**, *88*, 2692–2696.
9. (a) Vane, J. R.; Botting, R. M. *Inflammation Res.* **1998**, *47*, S78–S87; (b) Katori, M.; Majima, M.; Harada, Y. *Inflammation Res.* **1998**, *47*, S107–S111.
10. DeWitt, D. L. *Mol. Pharmacol.* **1999**, *55*, 625.
11. Penning, T. D.; Talley, J. J.; Bertenshaw, S. R.; Carter, J. S.; Collins, P. W.; Docter, S.; Graneto, M. J.; Lee, L. F.; Malecha, J. W.; Miyashiro, J. M.; Rogers, R. S.; Rogier, D. J.; Yu, S. S.; Anderson, G. D.; Burton, E. G.; Cogburn, J. N.; Gregory, S. A.; Koboldt, C. M.; Perkins, W. E.; Seibert, K.; Veenhuizen, A. W.; Zhang, Y. Y.; Isakson, P. C. *J. Med. Chem.* **1997**, *40*, 1347.

12. (a) Texier-Boullet, F.; Klein, B.; Hamelin, J. *Synthesis* **1986**, 409; (b) Sreekumar, R.; Padmakumar, R. *Synth. Communun.* **1998**, *28*, 1661; (c) Wang, Z.; Qin, H. *Green Chem.* **2004**, *6*, 90–92, and references cited therein.
13. (a) Lee, K. Y.; Gowrisankar, S.; Kim, J. N. *Tetrahedron Lett.* **2005**, *46*, 5387; (b) Dvorak, C. A.; Rudolph, D. A.; Ma, S.; Carruthers, N. I. *J. Org. Chem.* **2005**, *70*, 4188; (c) Lee, K. Y.; Kim, J. M.; Kim, J. N. *Tetrahedron Lett.* **2003**, *44*, 6737.
14. Curini, M.; Rosati, O.; Campagna, V.; Montanari, F.; Cravotto, G.; Boccalini, M. *Synlett* **2005**, *19*, 2927.
15. Curini, M.; Rosati, O.; Costantino, U. *Curr. Org. Chem.* **2004**, *8*, 591.
16. Morris, G. M.; Goodsell, D. S.; Halliday, R. S.; Huey, R.; Hart, W. E.; Belew, R. K.; Olson, A. J. *J. Comput. Chem.* **1998**, *19*, 1639.
17. Kurumbail, R. G.; Stevens, A. M.; Gierse, J. K.; McDonald, J. J.; Stegeman, R. A.; Pak, J. Y.; Gildehaus, D.; Iyashiro, J. M.; Penning, T. D.; Seibert, K.; Isakson, P. C.; Stallings, W. C. *Nature* **1996**, *384*, 644.
18. Liu, H.; Huang, X.; Shen, J.; Luo, X.; Li, M.; Xiong, B.; Chen, G.; Shen, J.; Yang, Y.; Jiang, H.; Chen, K. *J. Med. Chem.* **2002**, *45*, 4816.
19. Price, M. L.; Jorgensen, W. L. *Bioorg. Med. Chem. Lett.* **2001**, *11*, 1541.
20. Lipinski, C. A.; Lombardo, F.; Dominy, B. W.; Feeney, P. J. *Adv. Drug Delivery Rev.* **2001**, *46*, 3.
21. Clark, D. E.; Pickett, S. D. *Drug Discovery Today* **2000**, *5*, 49.
22. Palm, K.; Stenberg, P.; Luthman, K.; Artursson, P. *Pharm. Res.* **1997**, *14*, 568.
23. Butler, S. H.; Godefroy, F.; Besson, J. M.; Weil-Fugazza, J. *Pain* **1992**, *48*, 73.
24. Besson, J. M.; Guilbaud, G. *Excerpta Medica*; Elsevier: Amsterdam, 1988, 257.
25. Calvino, B.; Crepon-Bernard, M. A.; Le Bars, D. *Behav. Brain Res.* **1987**, *24*, 11.
26. Winter, C. A.; Risley, E. A.; Nuss, G. W. *Proc. Soc. Exp. Biol. Med.* **1962**, *111*, 544.
27. Solano, R.; Herrero, J. F. *Neuroscience* **1999**, *90*, 1393.
28. Coulthard, P.; Simjee, S. U.; Pleuvry, B. J. *J. Neurosci. Methods* **2003**, *128*, 95.
29. Lolli, M. L.; Cena, C.; Medana, C.; Lazzarato, L.; Morini, G.; Corazzi, G.; Manarini, S.; Fruttero, R.; Gasco, A. *J. Med. Chem.* **2001**, *44*, 3463.
30. Srivastava, R. M.; de Almeida Lima, A.; Viana, O. S.; da Costa Silva, M. J.; Catanho, M. T.; de Morais, J. O. *Bioorg. Med. Chem.* **2003**, *11*, 1821.
31. Kato, S.; Ogawa, Y.; Kanatsu, K.; Okayama, M.; Watanabe, T.; Arakawa, T.; Takeuchi, K. *J. Pharmacol. Exp. Ther.* **2002**, *303*, 503.
32. Kato, S.; Takeuchi, K. *Jpn. J. Pharmacol.* **2002**, *89*, 1.
33. Holzer, P.; Lippe, I. T. H. *Neuroscience* **1988**, *27*, 981.
34. Gardmark, M.; Hoglund, A. U.; Hammarlund-Udenaes, M. *Pharmacol. Toxicol.* **1998**, *83*, 252.
35. Accelrys Cerius-2, Insight-II: San Diego, CA.
36. Rappe, A. K.; Casewit, C. J.; Colwell, K. S.; Goddard, W. A.; Skiff, W. M. . *J. Am. Chem. Soc.* **1992**, *114*, 10024.
37. Sanner, M. F. *J. Mol. Graphics Modell.* **1999**, *17*, 57.
38. ChemAxon Jchem: Maramaros koz 3/a, Budapest, 1037 Hungary.